Brazilian Journal of Chemical Engineering (2024) 41:633–642
https://doi.org/10.1007/s43153-023-00311-4

ORIGINAL PAPER

Structural characterization of asphaltenes enriched in Island and archipelago motifs by LDI (+) FT-ICR MS

Lidya C. Silva[1] · Jeferson V. Dávila[1] · Jussara V. Roque[1] · Flávio O. Sanches-Neto[1] · Rosineide C. Simas[1,2] · Felipe P. Fleming[3] · Boniek G. Vaz[1]

Received: 30 September 2022 / Revised: 31 January 2023 / Accepted: 4 March 2023 / Published online: 23 March 2023

Abstract
Fourier transform ion cyclotron resonance mass spectrometers (FT-ICR MS) play a major role due to their capability to provide information at the molecular level of complex samples. However, asphaltenes deposition in capillaries during ionization hinders the analysis of unstable fractions. To overcome this, in our previous work (10.1016/j.fuel.2022.124418), we demonstrated laser desorption ionization (LDI) as an alternative to FT-ICR MS analysis of unstable asphaltene fractions without the occurrence of any capillary obstructions. Herein, a simplified fractionation methodology for separating asphaltene fractions according to their structural motifs is presented. Then, the asphaltene fractions were characterized by LDI (+) FT-ICR MS. Moreover, structural characterization was also performed Collision-Induced Dissociation (CID) experiments.

Keywords Asphaltenes structures · Asphaltene characterization · Mass Spectrometry · Asphaltenes fractionation

Introduction

Asphaltenes are the petroleum fraction insoluble in n-alkanes, but soluble in toluene (Podgorski et al. 2013; Rueda-Velásquez et al. 2013; Santos et al. 2014). The asphaltene molecules can be classified as island or archipelago-type. The island-type molecules are constituted by a single polycondensed aromatic nucleus. On the other hand, archipelago-type asphaltenes consist of at least two aromatic nuclei linked by alkyl bridges (Chacón-Patiño et al. 2017).

This petroleum fraction is known as the responsible for several problems in the oil industry, such as deposit formation in wells, pipes, and reservoirs (Ghosh et al. 2016; Neuhaus et al. 2019; Subramanian et al. 2016). Therefore, it is essential to characterize asphaltenes, as the knowledge produced can be used to support models that allow us to predict under what conditions asphaltenes will remain stable (Dutta Majumdar et al. 2017; Mousavi-Dehghani et al. 2008; Rashid et al. 2019).

Mass spectrometers with FT-ICR analyzers are essential to accomplish this task, as they can differentiate thousands of species in mass spectra (Molnárné Guricza & Schrader 2015). Even so, the high complexity of asphaltene samples and its tendency to self-associate make their analysis a challenging task.

The high complexity of asphaltenes samples directly impacts MS analyses due to differences in ionization efficiencies. Consequently, only the most ionizable species are detected when analyzing such a complex sample (Chacón-Patiño et al. 2017, 2018). To overcome this problem, the fractionation of asphaltenes into sub-fractions of reduced complexity is normally employed.

However, the asphaltene's self-association tendencies are another problem to be concerned about. That is because asphaltenes tend to aggregate before and during ionization (Chacón-Patiño et al. 2017; Herod 2010; McKenna et al. 2013). That is specially concerning because the most common ion sources used for MS analysis of asphaltenes, electrospray ionization (ESI) and atmospheric pressure photon ionization (APPI), that require the complete solubilization of the sample. Therefore, this can make it unfeasible to analyze asphaltene fractions that show greater aggregation tendencies.

✉ Boniek G. Vaz
boniek@ufg.br

[1] Institute of Chemistry, Federal University of Goiás, Goiânia, Goiás, Brazil

[2] School of Engineering, Mackenzie Presbyterian University, São Paulo, São Paulo, Brazil

[3] Petróleo Brasileiro S.A, CENPES, Rio de Janeiro, Rio de Janeiro, Brazil

Alternatively, in a previous study we demonstrated Laser Ionization/Desorption (LDI) as a viable tool for the FT-ICR MS characterization of asphaltenes in solid state without the occurrence of capillary obstructions. Herein, a fractionation methodology based on solubility mechanisms is presented. Then, all asphaltene fractions were characterized by LDI (+) FT-ICR MS analyses and the structural characterization of the samples was achieved by CID experiments.

Materials and methods

Materials

The HPLC grade (≥ 99%) n-heptane (Hep), ≥ 99% purity used in precipitation and extraction was purchased from Sigma Aldrich (Saint Louis, USA). The HPLC grade (≥ 99%) acetone, acetonitrile (ACN), and toluene (Tol) were purchased from Tedia (Fairfield, USA). The glass microfibre filters (90 mm) used were purchased from Whatman (Maidstone, UK).

Separation of C-7 asphaltenes

Asphaltenes were precipitated from two Brazilian oils as previously described (Silva et al. 2022). Briefly, n-heptane (n-C_7) was added to the samples in proportions of 40 mL for each 1 g of oil. The mixtures were subject to ultrasonic bath for 60 min and left to stand for 24 h. Then, filtration was performed with glass fiber membranes for the separation of the unclean asphaltenes from the soluble fraction (maltenes). Finally, the unclean asphaltenes were washed with n-C_7 in a Soxhlet apparatus for 120 h to promote the removal of occluded compounds.

Asphaltenes fractionation

The purified asphaltenes were encapsulated in chromatographic filter paper and inserted into the Soxhlet apparatus for the extraction of 5 fractions using acetone, ACN, Hep, Hep/Tol (1:1), and Tol. The extraction process for each fraction lasted for 24 h and 250 mL of each eluent was used to obtain the samples. The sample was ground between each extraction step to increase its area surface, improving extraction efficiency. Photos of the obtained fractions and a fractionation procedure scheme are shown in Fig. 1S.

Asphaltenes characterization by LDI (+) FT ICR MS

Analyses were performed using positive-ion mode LDI on a SolariX FT-ICR MS (Bruker, Germany) equipped with a YAG laser (355 nm) as previously described (Silva et al. 2022). For this, all samples were dissolved in toluene at a concentration of 1 $mg.mL^{-1}$ and 1 µL of each solution was spotted on the stainless-steel target without matrix. After drying, the LDI (+) FT-ICR MS spectra were acquired with laser power from 17 to 24% and from 15 to 400 laser shots, according to the ionization efficiency of the analyzed sample.

Moreover, CID experiments were performed for all asphaltene subfractions in 3 different ranges of m/z (375, 428 and 515 ± 20 Da). For this, a collision energy of 30 V (Q1 CID Energy) was employed for the range of m/z 375 ± 20 Da range while 40 V was employed in CID experiments performed for the ranges of m/z 428 and 515 ± 20 Da.

Data processing

Data visualization was performed with Bruker Compass DataAnalysis 5.0 software, and molecular formula assignments were performed with Composer 1.0.6 software. Finally, the graphs were plotted using the Software Microsoft Excel, OriginPro 2018 b9.5.1.195, and Thanus 1.0.

Calculation methods

The molecular structures were characterized using analytical harmonic frequency calculations at the B3LYP/6–31 + G(d) level. The absence of an imaginary frequency indicates that the optimized structure is a local minimum (Sanches-Neto et al. 2020). The quantum chemistry calculations reported in this study were performed using the Gaussian 09 computational package (Frisch et al. 2016).

Results and discussion

Asphaltenes fractionation

Initially, a Brazilian asphaltene sample was fractionated by solubility mechanisms by Soxhlet extraction using a series of solvents: acetone, acetonitrile, heptane, heptane/toluene (1:1 v/v) and toluene. The same asphaltene sample was already characterized by LDI (+) FT-ICR MS and the results were reported in our previous study (Silva et al. 2022).

Tab. 1S shows the percentage yield of each sample extracted, and the total recovery. As already reported, acetone is employed for the separation of asphaltene fractions that presents high ionization efficiency in positive-ion mode for LDI and APPI (Chacón-Patiño et al. 2018; Rodgers et al. 2019; Silva et al. 2022). Then, acetonitrile is used to remove porphyrins that may be present in the samples (Chacón-Patiño et al. 2018; Giraldo-Dávila et al. 2016). Using these solvents is important for the separation of the easily ionizable species that causes ion suppression in MS analysis, limiting the complete characterization of asphaltenes samples.

Extractions with acetone and acetonitrile fractions resulted in recovery yields lower than 1%, which can be explained by the low solubility of asphaltenes in these solvents (Larichev et al. 2016; Morantes et al. 2019). On the other hand, 5.8% of the sample was extracted using heptane. Although asphaltenes are insoluble in n-alkanes, in Soxhlet systems it is possible to extract low polarity asphaltene (Chacón-Patiño et al. 2016, 2018; Juyal et al. 2013; Strausz et al. 2006). Besides, as asphaltenes have low solubility in acetone, acetonitrile, and heptane, Soxhlet extraction with these solvents will promote the removal of less insoluble compounds.

In the sequence, the use of the heptane/toluene (1:1 v/v) resulted in the extraction of 78.6% of the sample. After that, the asphaltenes species that remained insoluble were extracted with toluene. As asphaltenes are soluble in toluene, this behavior can be explained by the presence of 50% toluene in the Hep-Tol mixture. Even so, species with a greater tendency to aggregation remain insoluble, requiring a higher percentage of toluene (Chacón-Patiño et al. 2016; Gawrys et al. 2003; Santos Silva et al. 2019; Sedghi et al. 2013; Spiecker et al. 2003).

Our previous study demonstrated a relation between ionization efficiency (IE) and the number of laser shots (LS) required to ionize the samples (Silva et al. 2022). As seen in Eq. (1), the IE is lower the higher the number of LS needed to accumulate a target number of ions in MS analyses.

$$IE \propto \frac{1}{LS} \tag{1}$$

Equation 1 was used to calculate the IE for all analyzed samples. Afterward, the calculated IE values were compared with the mass recovery for each fraction. The results are presented in Fig. 1.

Note that fractions extracted with acetone and heptane showed the highest ionization efficiencies in LDI (+). On the other hand, despite the high mass recovery, samples extracted in Hep/Tol (1:1 v/v) and toluene are less ionizable. Thus, this result emphasizes the importance of the fractionation of asphaltenes because in analyzes of the unfractionated sample, only a small portion of the species would have their ionization favored.

The H/C ratios for the asphaltene sample determined by combustion elemental analysis is compared to the H/C ratio determined through LDI (+) FT-ICR MS analysis in Fig. 2. As seen, determining the H/C ratio from the LID (+) FT-ICR MS analysis results in lower H/C values as the LDI favors the ionization of hydrogen-deficient species. However, the H/C values derived from LDI (+) FT-ICR MS analysis of the fractions, calculated by Eq. (2), are higher. This result shows that the fractionation mitigates selective ionization. This is similar to the results published

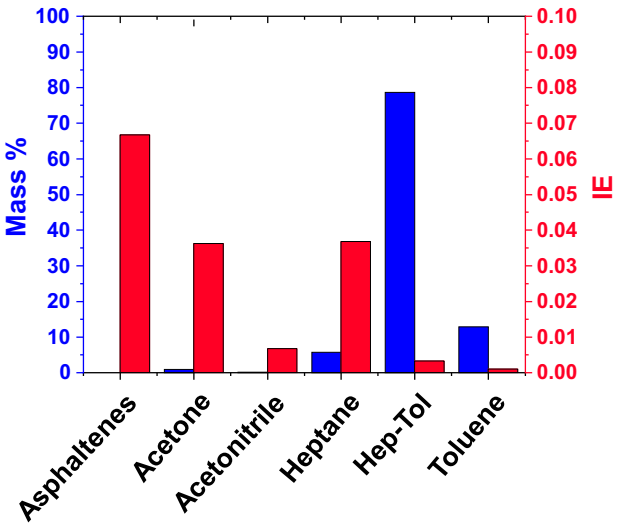

Fig. 1 Percentage of mass recovery and ionization efficiency for whole asphaltenes and asphaltene fractions

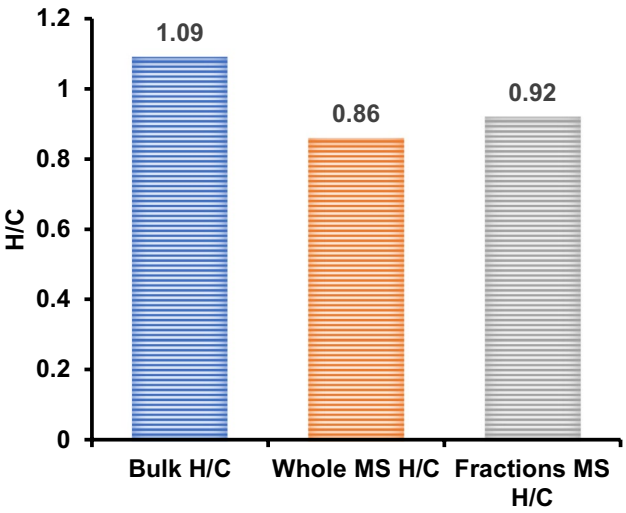

Fig. 2 Bulk H/C ratios and LDI (+) FT-ICR MS derived abundance-weighted H/C ratios for the whole asphaltene and the asphaltene fractions

by Chacón-Patiño et al. (2021), in which an extrography fractionation also enabled access to compounds of higher H/C ratios in APPI (+) FT-ICR MS analysis (Chacón-Patiño et al. 2021).

$$H/C_{Fractions} = \sum AWH/C_i \times wt\%_i \tag{2}$$

in which, the H/C ratios for the asphaltene fractions ($H/C_{Fractions}$) is equal to the sum of the abundance-weighted H/C ratio for each fraction (AW H/C_i) versus the percentual recovery of each extracted fraction ($wt\%_i$) (Chacón-Patiño et al. 2021).

Characterization of the asphaltene fractions

Figure 3 illustrates the LDI (+) FT-ICR MS spectra and the class distribution of the five asphaltene fractions extracted by the fractionation method. Detailed information on the mass spectra, such as zoom insets and peaks resolution relative to some assigned species, are shown in the supplementary material (from Fig. 2S to Fig. 6S). In addition, Table 2S shows information about the processing performance, i.e., the number of peaks and percentage of assigned species. Plus, error distributions for the molecular assignments are shown in Fig. 7S.

In the spectra of Fig. 3a, the samples extracted with acetone, acetonitrile, and heptane showed unimodal distributions. On the other hand, samples extracted with Hep-Tol, and toluene showed greater amplitudes of m/z distribution and non-uniform profile, suggestive of the occurrence of nano-aggregation during the ionization process.

In Fig. 3b, it is seen a greater abundance of oxygen and sulfur-containing compounds in the last two fractions. Such results agree with the hypothesis of dimer and nano-aggregates formation during the ionization of Hep-Tol and Toluene samples, since, in asphaltenes, a greater content of acidic species is related to higher aggregation tendencies (Juyal et al. 2010; Pinto et al. 2017; Rodgers and McKenna 2011).

As seen in Fig. 2 (b), hydrocarbons and nitrogen-compounds were detected in greater abundance in the LDI (+) FT-ICR MS analyses. Figure 4 shows the double-bound equivalent (DBE) distributions versus carbon numbers (C#) with mean values for the DBE and H/C ratios calculated for these compounds. In addition, DBE x #C relative to acidic compounds containing O and S heteroatom were also included, as they seem to play an important role in the asphaltenes aggregation.

Note that samples extracted with acetone and acetonitrile reached lower DBE values. On the other hand, it was detected highly unsaturated species (DBE > 40) in the heptane/toluene and toluene extracted samples, especially for the O and S-containing compounds.

The H/C ratios are indicators of aromaticity, in which a low H/C average suggests a greater aromaticity. For the N-compounds, H/C is higher for acetone, acetonitrile, and heptane fractions, contrasting with the Heptane, Hep-Tol, and Toluene fractions, where compounds with higher C# and DBE were detected. Likewise, the HC compounds detected in the Hep-Tol, and Toluene fractions exhibit similar compositional spaces. Thus, we can affirm that more aromatic species were extracted in these last two fractions.

Finally, for the sample extracted in toluene, the O and S-containing compounds exhibit an atypical compositional space, in which, most of the compounds are in a region of DBE > 40. In addition, a bimodal profile evidence the presence of asphaltene aggregates in this sample. Therefore, the results suggest a higher aggregation tendency for the O and S heteroatom containing compounds extracted in toluene. Such results agree with other studies published

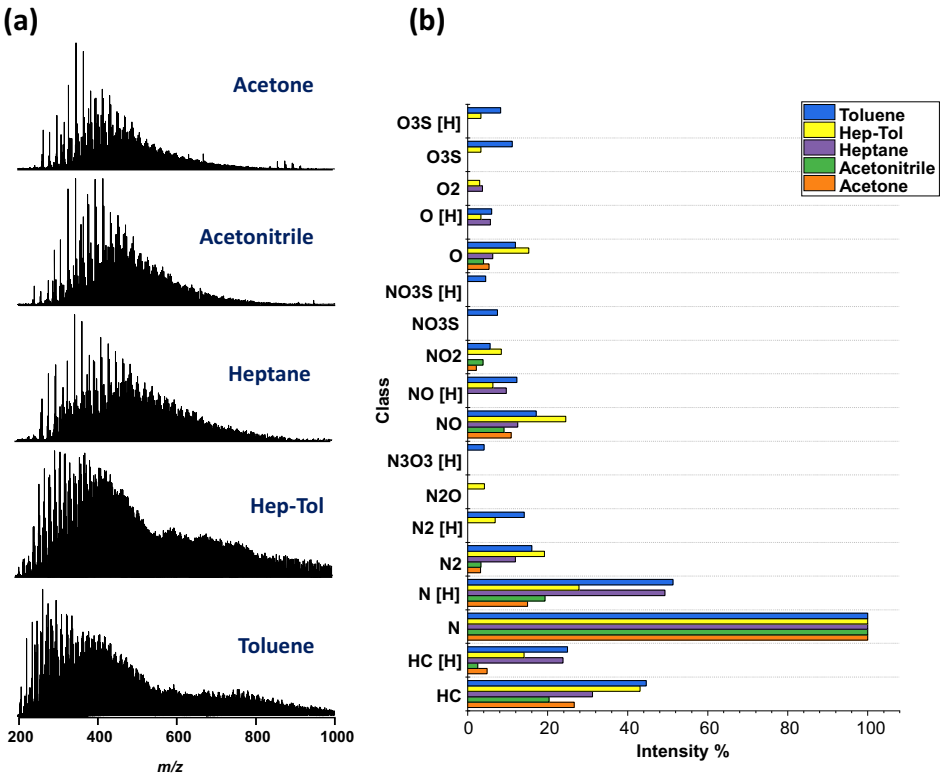

Fig. 3 (**a**) LDI (+) FT-ICR MS spectra and (**b**) class distribution bar graph for the most abundant heteroatomic classes detected in the asphaltene F-01 subfractions extracted by the developed methodology using acetone, acetonitrile, heptane, heptane/toluene (1:1 v/v), and toluene

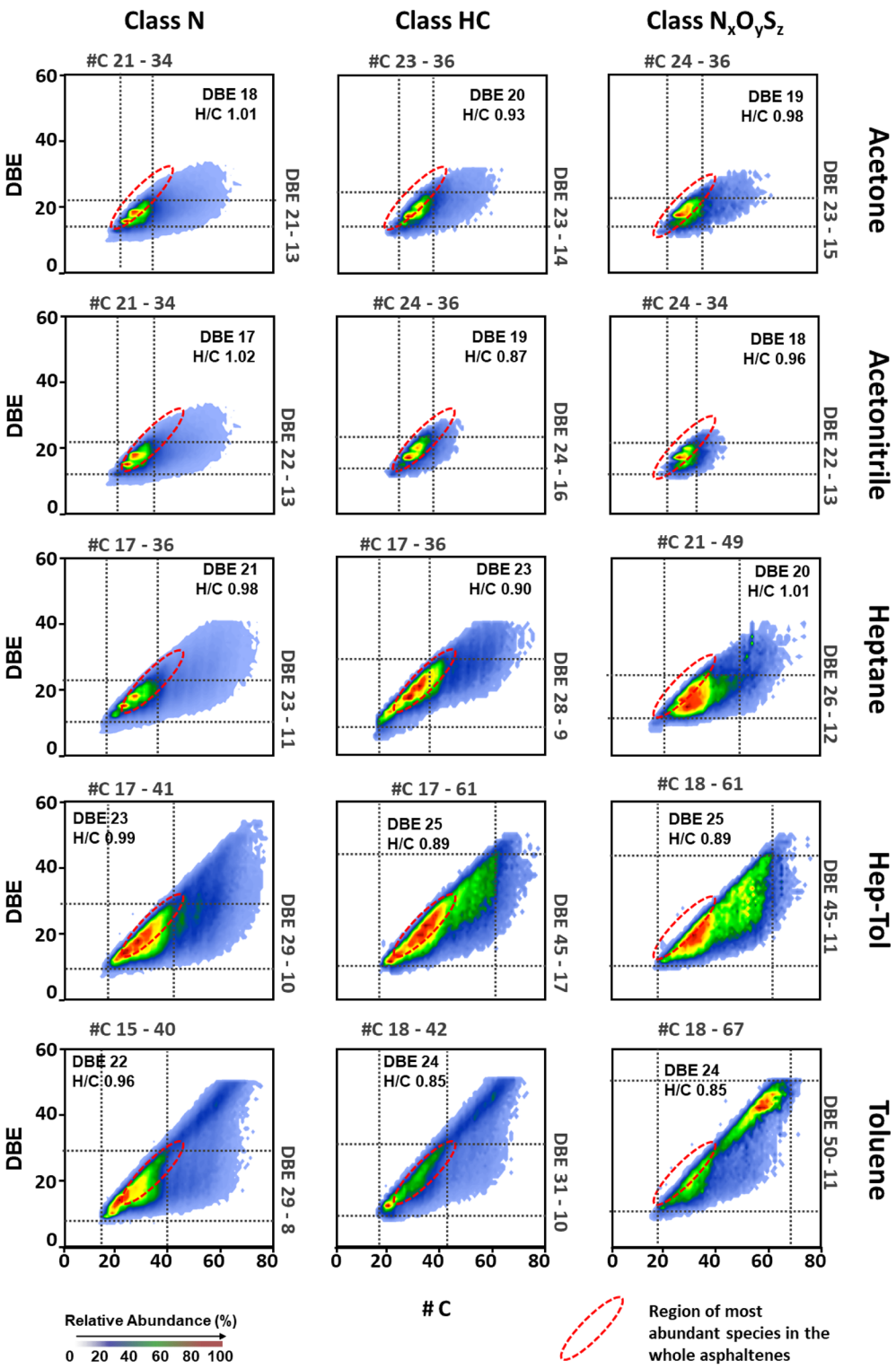

Fig. 4 Graphs of DBE versus carbon numbers, average DBE and H/C for N and HC class compounds, and classes containing heteroatoms O and S detected in the LDI (+) FT-ICR MS analysis of the asphaltene fractions

Table 1 Planar limit slops for the compounds of class N, HC, and $N_xO_yS_z$ detected in the asphaltene fractions

Fraction	Class N	Class HC	Class $N_xO_yS_z$
Acetone	0.696	0.740	0.623
Acetonitrile	0.685	0.717	0.685
Heptane	0.709	0.742	0.721
Heptane/Toluene	0.872	0.827	0.759
Toluene	0.892	0.904	0.810

Table 2 Aromaticity indices calculated for the compounds of class N, HC, and $N_xO_yS_z$ detected in the asphaltene fractions

Fraction	Class N	Class HC	Class $N_xO_yS_z$
Acetone	1.896	1.802	1.855
Acetonitrile	1.885	1.693	1.780
Heptane	1.860	1.762	1.919
Heptane/Toluene	1.864	1.748	1.745
Toluene	1.799	1.678	1.668

in the literature. In this case, the presence of these heteroatoms contributes to the formation of polar interactions between asphaltenes molecules, thus, aggregation is favored (Chacón-Patiño et al. 2020; Kilpatrick 2012).

Planar limits are defined as lines connecting maximum DBE values at given carbon numbers. Analyzing the slopes and y-intercepts of these lines is a means of predicting structure and molecular condensation. For asphaltenes, high planar limit slopes (~0.90) are associated with peri-condensed structures resulting from the non-linear addition of benzene units. On the other hand, the cata-condensed structures, resulting from the linear addition of benzene units, show planar limits slopes close to 0.75 (Cho et al. 2011; Hsu et al. 2011; Silva et al. 2022). The planar limit slopes for the compounds of class N, HC, and $N_xO_yS_z$ detected in the asphaltene fractions are shown in Table 1.

The higher slopes for samples extracted in heptane/toluene and toluene indicate the predominance of peri-condensed structures. On the other hand, the first three fractions are mostly composed of cata-condensed structures.

Furthermore, the carbon number per DBE ratio (#C / DBE) acts as an aromaticity indicator. In this regard, low #C/DBE ratios indicate increased aromaticity. Aromaticity indices calculated for compounds of classes N and HC and other classes containing O and S heteroatoms are presented in Table 2 For all classes, the results show the greater aromaticity of the compounds extracted in heptane/toluene and toluene. Such results agree with the H/C ratios shown in Fig. 3.

Structural characterization of the asphaltene fractions

CID experiments can be used in the structural characterization of asphaltenes, differentiating fractions enriched in island and archipelago motifs (Silva et al. 2022). In this, the cleavage of alkyl bridges between aromatic cores reveals the presence of archipelago structures. To perform this, the region of m/z 428 ± 10 Da was selected, and the resulting LDI (+) FT-ICR MS/MS spectra are shown in Fig. 5 along

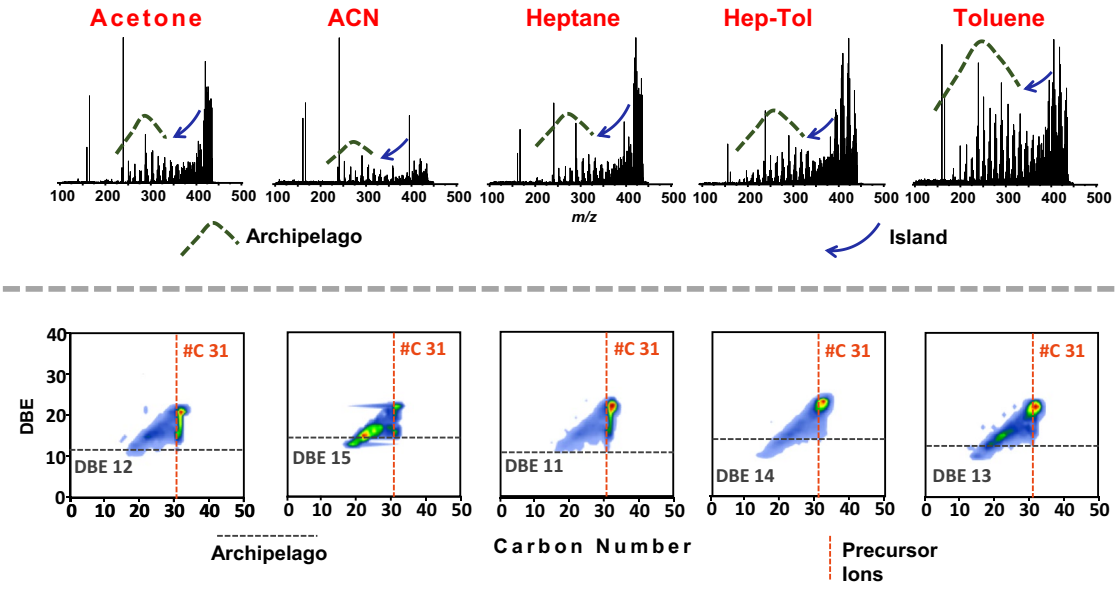

Fig. 5 Product ion mass spectra for m/z 428 ± 10 Da from LDI (+) FT-ICR MS/MS analyzes of the asphaltene fractions along with the resulting DBE x C# plots

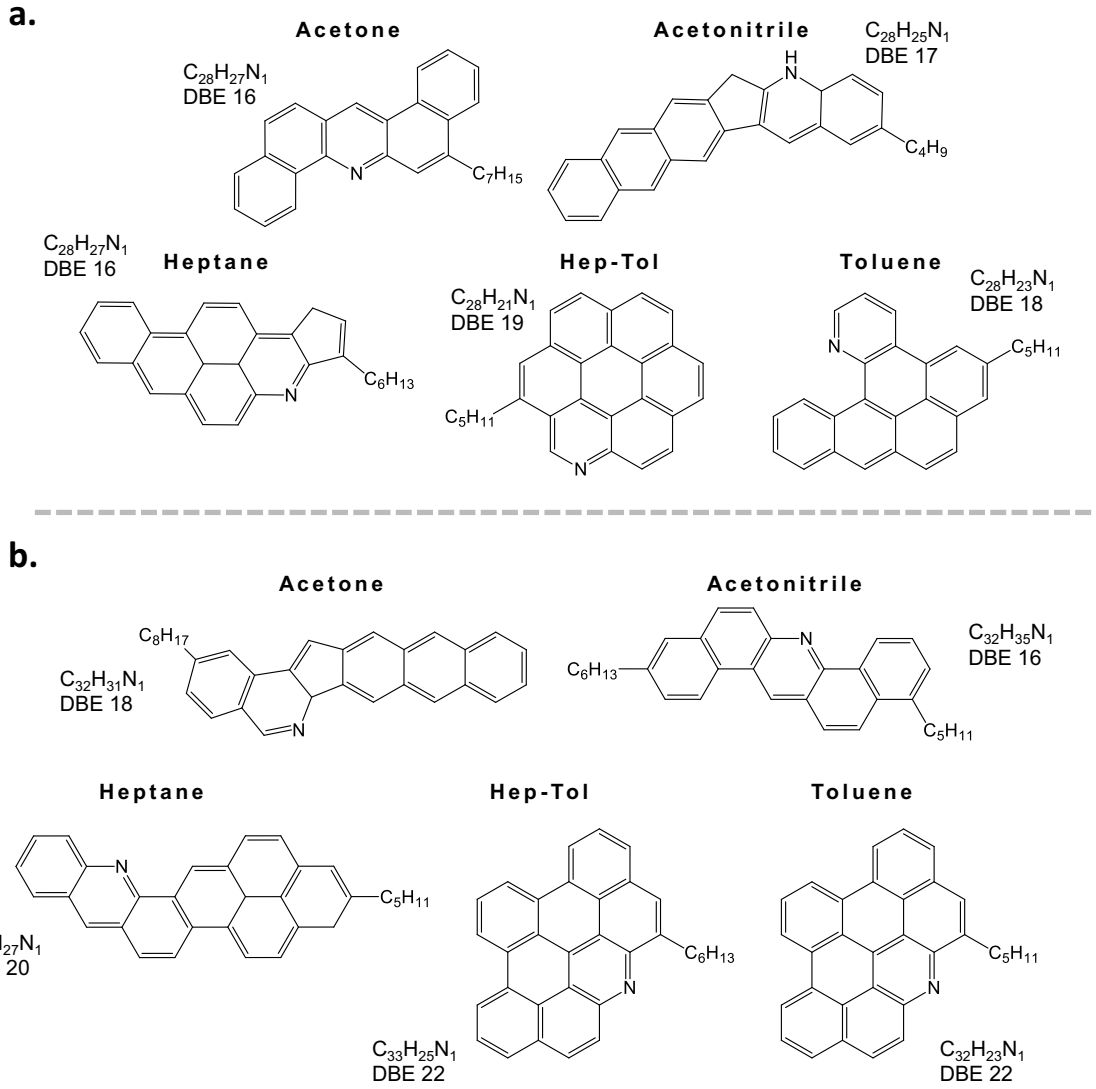

Fig. 6 Theoretical structures proposed for the most abundant and representative molecular formulas identified in the fractions in the ranges of (**a**) m/z 375 and (**b**) 428 ± 10 Da

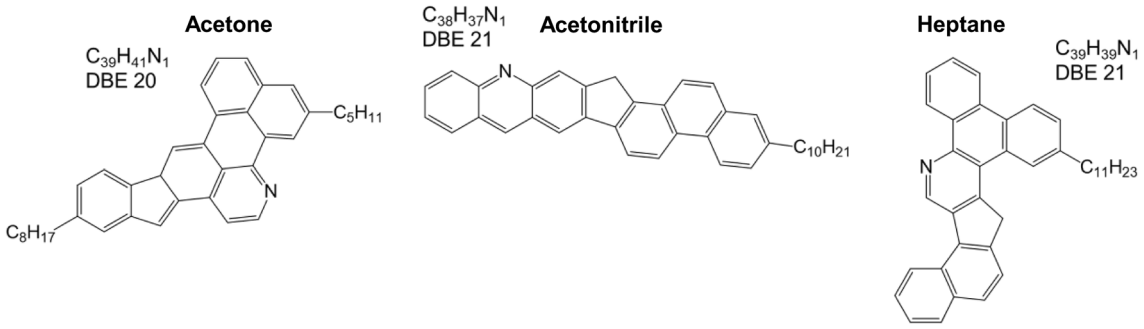

Fig. 7 Theoretical structures proposed for the most abundant and representative molecular formulas identified in the fractions extracted in acetone, acetonitrile, and heptane for m/z 515 ± 10 Da

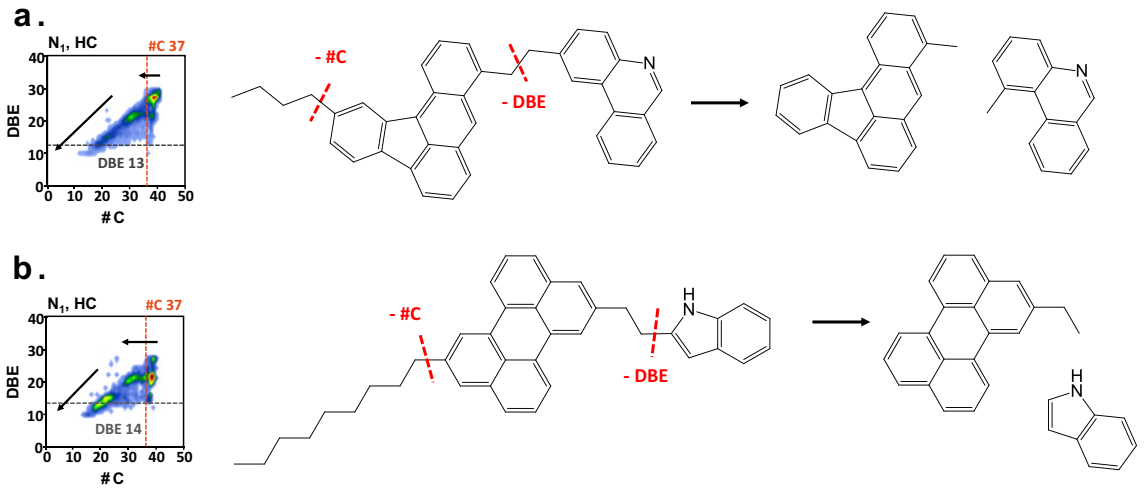

Fig. 8 Plots of DBE versus carbon number and theoretical structures proposed for the most abundant and representative molecular formulas identified in the fractions extracted with (**a**) heptane/toluene, and (**b**) toluene in the range of m/z 515 ± 10 Da

with plots of DBE x #C for each fraction. The error distributions for the molecular assignments are presented in supplementary material (from Fig. 8S to Fig. 10S).

In the LDI (+) FT-ICR MS/MS spectra, only dealkylation profiles are seen in the dissociation of island-type asphaltenes. In contrast, the cleavage of alkyl bridges between aromatic cores in archipelago-type asphaltenes leads to the formation of low m/z fragments. Consequently, in MS/MS spectra, a bimodal profile is suggestive of a greater abundance of archipelago-type asphaltenes. Therefore, the mass spectra seen in Fig. 5 suggest the predominance of archipelago-type asphaltenes in the fraction extracted with toluene.

Graphs of DBE x C# are also presented in Fig. 5. In the graphs, vertical lines have been drawn to separate the region of precursors and product ions while horizontal lines indicate the lowest DBE of the precursors. Therefore, only fragments derived from the cleavage of alkyl bridges between aromatic cores in archipelago structures will be found below this horizontal line.

For all samples, the precursor ions covered a wide range of DBE, therefore, most of the fragments are found in a region above the line that delimits the DBE of the precursors. So, it makes it difficult to verify the presence of archipelago structures by losses of aromaticity. Even so, the toluene-extracted sample seems to contemplate a greater content or archipelago-type asphaltenes. Meanwhile, the first three fractions apparently comprehend a lower content of archipelago-derived product ions. Also, these findings agree with the results of CID experiments for other mass ranges in which the toluene-extracted sample seems enriched in archipelago-type asphaltenes, regardless of the m/z range analyzed (see Fig. 2S and 3S).

Further, the data about DBE and the number of aliphatic carbons obtained by analyzing the dealkylation profiles made it possible the proposition of molecular structures for the asphaltenes species. Figure. 6 shows theoretical structures proposed for the most abundant ions detected in each fraction by LDI (+) FT-ICR MS/MS analyses for m/z 375 and 438 ± 10 Da.

For m/z 375 ± 10 Da, the ions detected in greater abundance in the fractions extracted with acetone and heptane have the same molecular formula. However, an in-depth analysis of the MS/MS data evidence the occurrence of structural isomerism due to the different numbers of aliphatic carbons in these structures. For the m/z 428 ± 10 Da, structures with the same aromatic nucleus were proposed for the most abundant species detected in the samples extracted in heptane/toluene and toluene.

The structures proposed represent only one of the several possibilities of molecular arrangements for the molecular formulas detected. Even so, the proposed structures agree with the calculated planar limit slopes, and aromaticity indexes (C#/DBE) for N_1 compounds detected in LDI (+) FT-ICR MS analyses as shown in Table 1 and 2, respectively.

Molecular structures were also proposed for the ions identified in the region of m/z 515 ± 10 Da. In Fig. 7, the results point to the presence of cata-condensed structures in the first three fractions, with predominance of fragmentation by alkyl-side chains cleavage. In contrast, the Hep-Tol and toluene fractions presented archipelago-like fragmentation profiles. Thus, archipelago-type structures were proposed for the last two fractions along with possible fragmentation routs in.

Figure 8 a exemplifies a possible fragmentation route for the ion detected in greater abundance in the Hep-Tol

fraction. The proposed structure contains a nitrogen in one of the aromatic nuclei connected by an alkyl bridge. Several fragmentation routes are possible for this structure, but for all of them, the cleavage of the alkyl bridge leads to low DBE fragments. Moreover, an in-depth analysis of the MS/MS reveals the loss of four aliphatic carbons, leading to the formation of the product ion $C_{35}H_{21}N^{\bullet+}$ (DBE 25). Further, the data point to the cleavage of the bond between the two aromatic nuclei, generating the fragments $C_{21}H_{14}{}^{\bullet+}$ (DBE 15) and $C_{14}H_{11}N^{\bullet+}$ (DBE 10)

For the toluene-extracted sample, an in-depth analysis of the fragmentation reveals the loss of nine aliphatic carbons that leads to the fragment ion $C_{20}H_{21}N^{\bullet+}$ (DBE 21). Further, the cleavage of the alkyl bridge between the aromatic nuclei in the archipelago structure leads to the formation of hydrocarbon detected in the spectra with the molecular formula $C_{21}H_{14}{}^{\bullet+}$ (DBE 15) as shown in Fig. 8b.

The results of frequency calculations can be used to determine the stability of a molecule or compound and help identify possible issues with the molecular structure. Electronic structure calculations were performed using the Gaussian 16 software to confirm the proposed structures in Fig. 6 and Fig. 7 are real. The results showed that all structures have positive harmonic frequencies, indicating that they are local minima and therefore real. The harmonic frequencies obtained are presented in the Supplementary Material (from Tab. S3 to S12).

Conclusions

The fractionation methodology was effective in separating fractions that exhibit high ionization efficiencies, thus proving to be able to extend the characterization of asphaltenes samples, allowing access to information on species that are difficult to ionize. Furthermore, LDI (+) FT-ICR MS analysis allowed the characterization of all asphaltene samples, even the most unstable ones. Additionally, CID experiments were performed to provide structural characterization of the fractions. It was observed that the method was also effective in separating asphaltenes according to their condensation and structural motifs. Finally, structures were proposed based on data acquired and frequency calculations were conducted using Gaussian 09 software to confirm the validity of the proposed structures.

Supplementary Information The online version contains supplementary material available at https://doi.org/10.1007/s43153-023-00311-4.

Author contributions LCS: conceptualization, formal analysis, investigation, methodology, writing original draft, review, and editing. JVD: conceptualization, formal analysis, investigation, methodology, writiting, review, and editing. JVR: data treatment, software. FOSN: formal analysis, software. RCS: investigation, project administration. FFF: conceptualization, methodology. BGV: conceptualization, funding acquisition, investigation, project administration, resources, supervision, writing, review, and editing.

Funding This study was funded by PETROBRAS/ANP, FAPEG, CAPES, and CNPq.

Data availability Data supporting the findings of this study are available within the article and its supplementary materials. Additionaly, raw data are available on request from the corresponding author, Vaz, B.G.

Declarations

Conflict of interest The authors declare that they have no conflict of interest.

References

Chacón-Patiño ML, Vesga-Martínez SJ, Blanco-Tirado C, Orrego-Ruiz JA, Gómez-Escudero A, Combariza MY (2016) Exploring occluded compounds and their interactions with asphaltene networks using high-resolution mass spectrometry. Energy Fuels 30(6):4550–4561. https://doi.org/10.1021/acs.energyfuels.6b00278

Chacón-Patiño ML, Rowland SM, Rodgers RP (2017) Advances in asphaltene petroleomics Part 1: asphaltenes are composed of abundant Island and archipelago Structural Motifs. Energy Fuels 31(12):13509–13518. https://doi.org/10.1021/acs.energyfuels.7b02873

Chacón-Patiño ML, Rowland SM, Rodgers RP (2018) Advances in asphaltene petroleomics part 2: selective separation method that reveals fractions enriched in Island and archipelago structural motifs by mass spectrometry. Energy Fuels 32(1):314–328. https://doi.org/10.1021/acs.energyfuels.7b03281

Chacón-Patiño ML, Smith DF, Hendrickson CL, Marshall AG, Rodgers RP (2020) Advances in asphaltene petroleomics part 4 compositional trends of solubility subfractions reveal that polyfunctional oxygen-containing compounds drive asphaltene chemistry. Energy and Fuels. https://doi.org/10.1021/acs.energyfuels.9b04288

Chacón-Patiño ML, Gray MR, Rüger C, Smith DF, Glattke TJ, Niles SF, Neumann A, Weisbrod CR, Yen A, McKenna AM, Giusti P, Bouyssiere B, Barrère-Mangote C, Yarranton H, Hendrickson CL, Marshall AG, Rodgers RP (2021) Lessons learned from a decade-long assessment of asphaltenes by ultrahigh-resolution mass spectrometry and implications for complex mixture analysis. In Energy and Fuels 35(20):16335–16376. https://doi.org/10.1021/acs.energyfuels.1c02107

Cho Y, Kim YH, Kim S (2011) Planar limit-assisted structural interpretation of saturates/aromatics/ resins/asphaltenes fractionated crude oil compounds observed by fourier transform ion cyclotron resonance mass spectrometry. Anal Chem 83(15):6068–6073. https://doi.org/10.1021/ac2011685

da Silva LC, Dávila JV, Fleming FP, Combariza MY, Vaz BG (2022) Laser desorption ionization and collision induced dissociastion as powerful tools for FT-ICR mass spectrometric characterization of asphaltene fractions enriched in island and archipelago motifs. Fuel. https://doi.org/10.1016/J.FUEL.2022.124418

Dutta Majumdar R, Montina T, Mullins OC, Gerken M, Hazendonk P (2017) Insights into asphaltene aggregate structure using ultrafast MAS solid-state1H NMR spectroscopy. Fuel. https://doi.org/10.1016/j.fuel.2016.12.082

Frisch, M. J., Trucks, G. W., Schlegel, H. B., Scuseria, G. E., Robb, M. A., Cheeseman, J. R., Scalmani, G., Barone, V., Petersson,

G. A., Nakatsuji, H., Li, X., Caricato, M., Marenich, A. v., Bloino, J., Janesko, B. G., Gomperts, R., Mennucci, B., Hratchian, H. P., Ortiz, J. V., Fox, D. J. (2016) Gaussian 16, Revision C.01.

Gawrys KL, Spiecker PM, Kilpatrick PK (2003) The role of asphaltene solubility and chemical composition on asphaltene aggregation. Pet Sci Technol. https://doi.org/10.1081/LFT-120018533

Ghosh AK, Chaudhuri P, Kumar B, Panja SS (2016) Review on aggregation of asphaltene vis-a-vis spectroscopic studies. In Fuel. https://doi.org/10.1016/j.fuel.2016.08.031

Giraldo-Dávila D, Chacón-Patiño ML, Orrego-Ruiz JA, Blanco-Tirado C, Combariza MY (2016) Improving compositional space accessibility in (+) APPI FT-ICR mass spectrometric analysis of crude oils by extrography and column chromatography fractionation. Fuel 185:45–58. https://doi.org/10.1016/J.FUEL.2016.07.096

Herod AA (2010) Limitations of mass spectrometric methods for the characterization of polydisperse materials. Rapid Communications Mass Spectrometry. https://doi.org/10.1002/rcm.4653

Hsu CS, Lobodin VV, Rodgers RP, McKenna AM, Marshall AG (2011) Compositional boundaries for fossil hydrocarbons. Energy Fuels 25(5):2174–2178. https://doi.org/10.1021/EF2004392

Juyal P, Yen AT, Rodgers RP, Allenson S, Wang J, Creek J (2010) Compositional variations between precipitated and organic solid deposition control (OSDC) asphaltenes and the effect of inhibitors on deposition by electrospray ionization fourier transform ion cyclotron resonance (FT-ICR) mass spectrometry. Energy Fuels 24(4):2320–2326. https://doi.org/10.1021/ef900959r

Juyal P, McKenna AM, Fan T, Cao T, Rueda-Velásquez RI, Fitzsimmons JE, Yen A, Rodgers RP, Wang J, Buckley JS, Gray MR, Allenson SJ, Creek J (2013) Joint industrial case study for asphaltene deposition. Energy Fuels 27(4):1899–1908. https://doi.org/10.1021/ef301956x

Kilpatrick PK (2012) Water-in-crude oil emulsion stabilization: review and unanswered questions. Energy Fuels 26(7):4017–4026. https://doi.org/10.1021/ef3003262

Larichev YV, Nartova AV, Martyanov ON (2016) The influence of different organic solvents on the size and shape of asphaltene aggregates studied via small-angle X-ray scattering and scanning tunneling microscopy. Adsorption Sci Tech 34(3):244–257. https://doi.org/10.1177/0263617415623440

McKenna, A. M., Marshall, A. G., Rodgers, R. P. (2013) Heavy petroleum composition 4 Asphaltene compositional space .Energy and Fuels 27 (3), 1257–1267 https://doi.org/10.1021/ef301747d

Molnárné Guricza L, Schrader W (2015) Electrospray ionization for determination of non-polar polyaromatic hydrocarbons and polyaromatic heterocycles in heavy crude oil asphaltenes. J Mass Spectrom 50(3):549–557. https://doi.org/10.1002/jms.3561

Morantes LR, Percebom AM, Mejía-Ospino E (2019) On the molecular basis of aggregation and stability of Colombian asphaltenes and their subfractions. Fuel 241:542–549. https://doi.org/10.1016/j.fuel.2018.12.028

Mousavi-Dehghani SA, Mirzayi B, Vafaie-Sefti M (2008) Polymer solution and lattice theory applications for modeling of asphaltene precipitation in petroleum mixtures. Braz J Chem Eng 25(3):523–534. https://doi.org/10.1590/S0104-66322008000300010

Neuhaus N, Nascimento PTH, Moreira I, Scheer AP, Santos AF, Corazza ML (2019) Thermodynamic analysis and modeling of brazilian crude oil and asphaltene systems: an experimental measurement and a pc-saft application. Braz J Chem Eng 36(1):557–571. https://doi.org/10.1590/0104-6632.20190361S20170575

Pinto FE, Barros EV, Tose LV, Souza LM, Terra LA, Poppi RJ, Vaz BG, Vasconcelos G, Subramanian S, Simon S, Sjöblom J, Romão W (2017) Fractionation of asphaltenes in n-hexane and on adsorption onto CaCO3 and characterization by ESI(+)FT-ICR MS: Part I. Fuel 210:790–802. https://doi.org/10.1016/J.FUEL.2017.09.028

Podgorski DC, Corilo YE, Nyadong L, Lobodin VV, Bythell BJ, Robbins WK, McKenna AM, Marshall AG, Rodgers RP (2013) Heavy petroleum composition 5 Compositional and structural continuum of petroleum revealed. Energy Fuels 27(3):1268–1276. https://doi.org/10.1021/ef301737f

Rashid Z, Wilfred CD, Gnanasundaram N, Arunagiri A, Murugesan T (2019) A comprehensive review on the recent advances on the petroleum asphaltene aggregation. J Petroleum Sci Eng Elsevier BV. https://doi.org/10.1016/j.petrol.2019.01.004

Rodgers RP, McKenna AM (2011) Petroleum analysis. Anal Chem 83(12):4665–4687. https://doi.org/10.1021/ac201080e

Rodgers RP, Mapolelo MM, Robbins WK, Chacón-Patiño ML, Putman JC, Niles SF, Rowland SM, Marshall AG (2019) Combating selective ionization in the high resolution mass spectral characterization of complex mixtures. Faraday Discussions. https://doi.org/10.1039/c9fd00005d

Rueda-Velásquez RI, Freund H, Qian K, Olmstead WN, Gray MR (2013) Characterization of asphaltene building blocks by cracking under favorable hydrogenation conditions. Energy Fuels 27(4):1817–1829. https://doi.org/10.1021/ef301521q

Sanches-Neto FO, Coutinho ND, Palazzetti F, Carvalho-Silva VH (2020) Temperature dependence of rate constants for the H(D) + CH4 reaction in gas and aqueous phase: deformed transition-state theory study including quantum tunneling and diffusion effects. Struct Chem 31(2):609–617. https://doi.org/10.1007/S11224-019-01437-3/TABLES/2

Santos RG, Loh W, Bannwart AC, Trevisan O (2014) An overview of heavy oil properties and its recovery and transportation methods. Braz J Chem Eng 31(3):571–590. https://doi.org/10.1590/0104-6632.20140313S00001853

Santos Silva H, Alfarra A, Vallverdu G, Bégué D, Bouyssiere B, Baraille I, Alfarra A, Vallverdu G, Bégué D (2019) Asphaltene aggregation studied by molecular dynamics simulations: role of the molecular architecture and solvents on the supramolecular or colloidal behavior. Petroleum Sci 16:669–684. https://doi.org/10.1007/s12182-019-0321-y

Sedghi M, Goual L, Welch W, Kubelka J (2013) Effect of asphaltene structure on association and aggregation using molecular dynamics. J Phys Chem B. https://doi.org/10.1021/jp401584u

Spiecker PM, Gawrys KL, Kilpatrick PK (2003) Aggregation and solubility behavior of asphaltenes and their subfractions. J Colloid Interface Sci 267:178–193. https://doi.org/10.1016/S0021-9797(03)00641-6

Strausz OP, Torres M, Lown EM, Safarik I, Murgich J (2006) Equipartitioning of precipitant solubles between the solution phase and precipitated asphaltene in the precipitation of asphaltene. Energy Fuels 20(5):2013–2021. https://doi.org/10.1021/ef060013j

Subramanian S, Simon S, Sjöblom J (2016) Asphaltene precipitation models: a review. J Dispersion Sci Technol. https://doi.org/10.1080/01932691.2015.1065418